

Active Brownian Motion in Two Dimensions

Urna Basu,¹ Satya N. Majumdar,¹ Alberto Rosso,¹ and Gr  gory Schehr¹

¹ *LPTMS, CNRS, Univ. Paris-Sud, Université Paris-Saclay, 91405 Orsay, France*

We study the dynamics of a single active Brownian particle (ABP) in a two-dimensional harmonic trap. The active particle has an intrinsic time scale D_R^{-1} set by the rotational diffusion with diffusion constant D_R . The harmonic trap also induces a relaxational time-scale μ^{-1} . We show that the competition between these two time scales leads to a nontrivial time evolution for the ABP. At short times a strongly anisotropic motion emerges leading to anomalous persistence/first-passage properties. At long-times, the stationary position distribution in the trap exhibits two different behaviours: a Gaussian peak at the origin in the strongly passive limit ($D_R \rightarrow \infty$) and a delocalised ring away from the origin in the opposite strongly active limit ($D_R \rightarrow 0$). The predicted stationary behaviours in these limits are in agreement with recent experimental observations.

Active particles form a class of nonequilibrium systems which are able to generate dissipative directed motion through self-propulsion and consuming energy from their environment [1–5]. Study of active particles is relevant in a wide variety of biological and soft matter systems ranging from bacterial motion [6, 7], cellular tissue behaviour [8], formation of fish schools [9, 10] as well as granular matter [11, 12] and colloidal surfers [13]. Recent years have seen a tremendous surge of research, both theoretical and experimental, on active matter e.g., the collective behaviour of active particles which include flocking [14, 15], clustering [13, 16, 17], phase separation [18–20] and the absence of a well defined pressure [21].

In a recent experiment, Janus swimmers were confined in a two-dimensional harmonic-like trap with the use of an acoustic tweezer and the stationary density was measured by varying the trap strength [22]. Strong signatures of activity were observed even in the dilute limit, with a crossover from a Gaussian-like stationary state, to a strongly active stationary state, where the particles cluster at the outskirts of the trap. The dilute limit corresponds to a collection of non-interacting Active Brownian Particles (ABP), each one performing an overdamped directed spatial motion at a fixed speed but with the direction undergoing a rotational diffusion [23]. Numerical studies of a single ABP, in presence of confining potentials, have also observed a similar crossover in the stationary state [24, 25].

Dynamical behaviour of active Brownian particles differ crucially from passive ones. For a ‘passive’ or ordinary Brownian particle, the presence of a harmonic trap of strength μ sets a relaxational time scale μ^{-1} . At times $t \ll \mu^{-1}$, the particle diffuses isotropically and for $t \gg \mu^{-1}$, a Gaussian (Boltzmann) stationary distribution is reached. For an ABP, the coupling to the rotational diffusion introduces an additional time scale D_R^{-1} , where D_R is the rotational diffusion constant.

While the activity induced crossover in the stationary position distribution of an ABP has been studied both experimentally and numerically, the interplay of the two time scales μ^{-1} and D_R^{-1} leads to fascinating dynamical features, already at the single particle level, that are yet to be explored. The aim of this Letter is to pro-

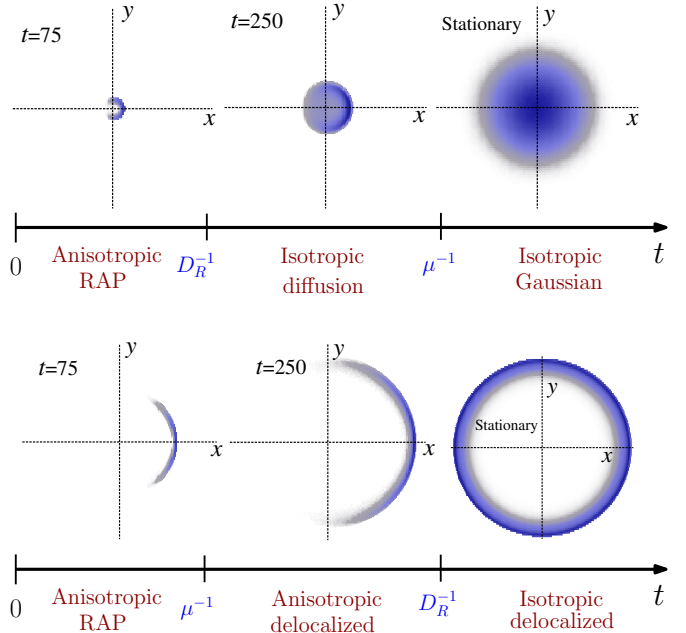


FIG. 1: Position probability distribution $P(x, y, t)$ for an ABP in a $2d$ harmonic trap of strength μ at different time t . Upper and lower panels correspond to the cases $\mu^{-1} > D_R^{-1}$ and $\mu^{-1} < D_R^{-1}$, respectively. The presence of anisotropy at short-times and the delocalized stationary state (for $\mu^{-1} < D_R^{-1}$) are both signatures of activity. The numerical data have been obtained with $D_R^{-1} = 10^2$ and $\mu^{-1} = 10^3$ (upper panel) and $D_R^{-1} = 10^3$ and $\mu^{-1} = 10^2$ (lower panel).

vide a detailed understanding of this dynamics, both the relaxation to the stationary state at late times, as well as the anomalous early time dynamics where anisotropy plays a dominant role. For the relaxational dynamics, we compute exactly the time dependent radial distribution function at all times, both in the strongly active ($D_R \rightarrow 0$) and strongly passive ($D_R \rightarrow \infty$) limit. For the early time dynamics, we establish an exact mapping to the “Random Acceleration Process” (RAP) and show that the ABP has anomalous non-Markovian persistence properties, with a nontrivial persistence exponent.

The physical picture emerging from our study is summarized in Fig. 1 for $D_R^{-1} < \mu^{-1}$ (upper panel) and for

$D_R^{-1} > \mu^{-1}$ (lower panel). In both cases, at short-times $t \ll \min(D_R^{-1}, \mu^{-1})$, the presence of activity gives rise to strong anisotropy with the particle keeping its initial orientation (chosen to be along x -direction here). In this regime, the effect of the trap can be neglected and we show that the evolution of the y -component maps onto the RAP, which is non-Markovian [28, 38]. At later times, if $D_R^{-1} < \mu^{-1}$, the anisotropy starts to disappear and the ABP undergoes ordinary diffusion (upper middle panel). Eventually, for $t \gg \mu^{-1}$ the probability distribution saturates to a Boltzmann-like form with a single Gaussian peak at the center of the trap. On the other hand, for strongly active system, *i.e.*, when $D_R^{-1} > \mu^{-1}$ the anisotropy persists and the particle starts to accumulate away from the center of the trap. For $t \gg D_R^{-1}$ the isotropy is slowly recovered (lower right panel). The stationary distributions we obtain in the two limiting cases are in agreement with the experimental and numerical observations [22, 25].

Model: We consider an active overdamped particle in the $2d$ -plane in the presence of a confining harmonic potential $U(x, y) = \mu(x^2 + y^2)/2$. In addition to its cartesian coordinates (x, y) the particles has an ‘active’ internal degree of freedom, given by the orientational angle $\phi(t)$ of its velocity, which undergoes rotational diffusion. The time evolution is encoded in the Langevin equation [3–5]

$$\dot{x} = -\mu x + v_0 \cos \phi(t) \quad (1a)$$

$$\dot{y} = -\mu y + v_0 \sin \phi(t) \quad (1b)$$

$$\dot{\phi} = \sqrt{2D_R} \eta_\phi(t). \quad (1c)$$

Here $\eta_\phi(t)$ is a Gaussian white noise with $\langle \eta_\phi(t) \eta_\phi(t') \rangle = \delta(t - t')$. D_R is the diffusion coefficient of the rotational degree of freedom. In principle, one could also add a translational thermal noise term to the (x, y) evolution. However, this only leads to a renormalisation of the effective diffusion constant [3–5], without changing the physics qualitatively. Hence we ignore this thermal noise. The self-propulsion, or ‘activity’, arises from the fact that the instantaneous linear velocity depends on the angle $\phi(t)$ with the constant speed v_0 controlling the strength of the coupling. We assume that the particle starts at the origin $x = y = 0$, oriented along x , *i.e.*, with angle $\phi = 0$. The angle $\phi(t)$ is just a standard Brownian motion with the auto-correlation $\langle \phi(t_1) \phi(t_2) \rangle = 2D_R \min\{t_1, t_2\}$.

It is convenient to consider the complex coordinate $z(t) = x(t) + iy(t)$ which evolves as

$$\dot{z} = -\mu z + \xi(t) \quad \text{where} \quad \xi(t) = v_0 e^{i\phi(t)}. \quad (2)$$

The magnitude of the effective noise $\xi(t)$ is clearly bounded, $|\xi(t)| \leq v_0$ at all times t . Consequently, the position of the particle also gets confined in a region $|z(t)| \leq r_b = v_0/\mu$ around the trap center. The noise $\xi(t)$ has an auto-correlation function [see the Supplemental Material (SM) [26] for details],

$$\langle \xi(t_1) \bar{\xi}(t_2) \rangle = v_0^2 \exp[-D_R|t_1 - t_2|], \quad (3)$$

where $\bar{\xi}(t) = v_0 e^{-i\phi(t)}$ is the complex conjugate of $\xi(t)$. Clearly, for times shorter than the persistence time $\tau_R = D_R^{-1}$, the noise $\xi(t)$ is strongly correlated.

Probability distribution: We are interested in the position probability distribution function (PDF) $P(x, y, t)$ in the $2d$ cartesian coordinates (or equivalently in $P(r, \theta, t)$ in the radial coordinates), especially its time evolution and approach to the stationary state. It can be obtained from $P(x, y, t) = \int \mathcal{P}(x, y, \phi, t) d\phi$ where $\mathcal{P}(x, y, \phi, t)$ is the PDF in both position and orientational coordinates. Starting from the Langevin equations (1), it is easy to write down the Fokker-Planck (FP) equation for $\mathcal{P}(x, y, \phi, t)$ (see [26]). Unfortunately, this FP equation is hard to solve, even for the stationary state. However, following an approach used in Ref. [27] in a different context, namely for the (imaginary) exponential functional of a Brownian motion, we were able to derive an exact evolution equation for the moments $M_{k,l}(t) = \langle z^k(t) \bar{z}^l(t) \rangle$ where $\bar{z}(t) = x(t) - iy(t)$ (see [26] for details). We get

$$\dot{M}_{k,l} = -D_R(k - l)^2 M_{k,l} + v_0 e^{-\mu t} [k M_{k-1,l} + l M_{k,l-1}], \quad (4)$$

with the initial condition $M_{k,l}(0) = 0$ for $k, l > 0$ and $M_{0,0}(t) = 1$ at all times. We also use the convention $M_{k,l}(t) = 0$ for $k, l < 0$. It is easy to check that $M_{k,l}(t) = M_{l,k}(t)$. Eq. (4) allows us to compute the moments explicitly in a recursive fashion (see [26] for the first few values of k, l). Using this moment evolution equation (4), it is possible to calculate the time-dependent radial distribution $P_{\text{rad}}(r, t) = \int_0^{2\pi} P(r, \theta, t) d\theta$ in the two limiting cases, $D_R \rightarrow \infty$ (strongly passive) and $D_R \rightarrow 0$ (strongly active). The details of the computation are provided in [26], here we quote only the main results.

In the limit $D_R \rightarrow \infty$, Eq. (4) can be solved explicitly at all times to obtain $M_{k,l}(t)$ for all k and l , to leading order in D_R^{-1} (see [26]). From these moments we infer the exact radial distribution function

$$P_{\text{rad}}(r, t) \simeq \frac{2 \mu D_R}{v_0^2 (1 - e^{-2\mu t})} \exp \left[-\frac{\mu D_R r^2}{v_0^2 (1 - e^{-2\mu t})} \right]. \quad (5)$$

Note that this solution is valid at all times t . In particular, at early times, when $D_R^{-1} \ll t \ll \mu^{-1}$ the solution in Eq. (5) corresponds to free isotropic diffusion with a diffusion constant $D_{\text{eff}} = v_0^2/2D_R$. This scenario corresponds to the upper middle panel in Fig. 1. In contrast, when $t \gg \mu^{-1}$, the radial distribution (5) approaches a stationary form. In addition, by analysing the decay of $M_{k,l}(t)$ for $k \neq l$, we find that the full position distribution becomes radially symmetric as $t \rightarrow \infty$. The stationary distribution is then given by $P_{\text{stat}}(x, y) = 1/(2\pi)P_{\text{rad}}(r, t \rightarrow \infty)$, a simple Gaussian centred at the origin. One thus recovers the Boltzmann distribution with an effective temperature $T_{\text{eff}} = v_0^2/2D_R = D_{\text{eff}}$, in full agreement with the experimental observation [22].

A very different scenario emerges in the strongly active limit $D_R \rightarrow 0$. Strictly for $D_R = 0$, Eq. (4) can be

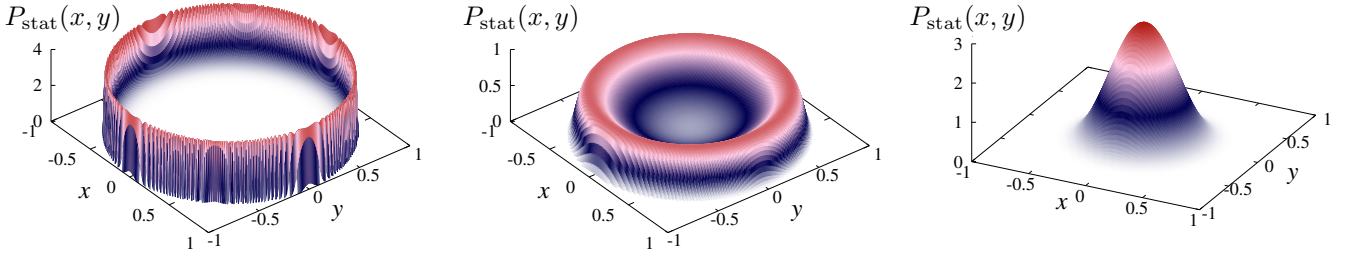


FIG. 2: Stationary distribution $P_{\text{stat}}(x, y)$ of an ABP in a harmonic trap for different values of $D_R = 0.1$ (left), $D_R = 1.0$ (centre) and $D_R = 10.0$ (right). The left and middle panel show the delocalized state where the particle is most likely to be accumulated away from the center. The right panel corresponds to the passive limit where the stationary distribution is Gaussian. Here the trap stiffness $\mu = 1.0$ and $v_0 = 1.0$.

solved exactly and this gives an exact time-dependent radial distribution [26]

$$P_{\text{rad}}(r, t) = \frac{\mu}{v_0(1 - e^{-\mu t})} \delta \left[r - \frac{v_0(1 - e^{-\mu t})}{\mu} \right]. \quad (6)$$

However, the full position distribution $P(x, y, t)$ is actually highly anisotropic [see Eq. (S54) in [26]]: due to the absence of rotational diffusion ($D_R = 0$), the particle keeps its initial orientation, even at late times. Hence, if one switches on a small $D_R = 0^+$, for times $t \ll D_R^{-1}$, the particle still keeps its initial orientation as for $D_R = 0$ (see middle panel of Fig. 1). However, for $t \gg D_R^{-1}$, the stationary distribution approaches an isotropic form: $P_{\text{stat}}(x, y) = \mu/(2\pi v_0) \delta \left[\sqrt{x^2 + y^2} - v_0/\mu \right]$ where the particle is strongly confined at the boundary of the trap $r_b = v_0/\mu$. This non-Boltzmann distribution results from the strongly active nature of the dynamics.

Figure 2 shows the stationary distribution $P_{\text{stat}}(x, y)$ in the (x, y) plane obtained from simulations, for different D_R . As D_R decreases, the stationary distribution shows a crossover from the passive regime, with a single-peaked Gaussian around $r = 0$, to the active regime, with a delocalized state where the particle is confined around a narrow ring away at $r_b = v_0/\mu$.

The marginal radial distribution $P_{\text{rad}}(r, t)$, being an integral over the angular degree of freedom, is inadequate to capture the anisotropy, present at early times, as visible from the simulations in the short-time regime (see Fig. 1). To investigate how this anisotropy evolves in time, we study the time-evolution of x and y components separately, focusing in particular on the moments and the first-passage properties. Since the anisotropy is most pronounced at early times $t \ll \mu^{-1}$, where the effect of the trap is negligible, we set $\mu = 0$ in the following. Starting from Eq. (1) with $\mu = 0$, we calculate, exactly for all t , the mean-squared displacements $\sigma_x^2 = \langle x^2 \rangle - \langle x \rangle^2$ (and similarly σ_y^2) [see Eq. (S23) in [26]]. In particular, at short times, we get

$$\begin{aligned} \sigma_x^2 &\approx \frac{1}{3} v_0^2 D_R^2 t^4 - \frac{7}{15} v_0^2 D_R^3 t^5 + \dots \\ \sigma_y^2 &\approx \frac{2}{3} v_0^2 D_R t^3 - \frac{5}{6} v_0^2 D_R^2 t^4 + \dots \end{aligned} \quad (7)$$

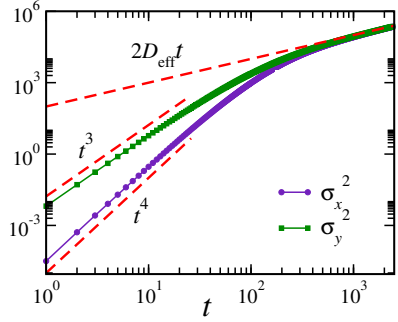


FIG. 3: Mean-squared displacement $\sigma_{x,y}^2$ of x and y components of the position of an ABP as a function of t for $v_0 = 1$ and $D_R = 0.01$. The symbols correspond to simulations and the solid lines are the predictions from the exact calculations.

This reflects a strong anisotropy at early times in the (x, y) plane: for small t , the fluctuations in the x -direction (the initial direction) $\sigma_x^2 \sim t^4$ are much smaller than in the y -direction $\sigma_y^2 \sim t^3$. Figure 3 compares the exact result of Eq. (S23) of [26] (solid lines) with the $\sigma_{x,y}^2$ obtained from simulations (symbols). At late times, $t \gg D_R^{-1}$ (with $\mu = 0$), both $\sigma_{x,y}^2 \approx 2D_{\text{eff}}t$ behave diffusively where $D_{\text{eff}} = v_0^2/2D_R$ [see Eq. (S23) in [26]].

To understand the evolution of the process at short times, we consider again the Langevin equations (1) with $\mu = 0$. At short times, $\phi(t) \sim \sqrt{t}$ is small. To leading order for small $\phi(t)$, $\cos \phi(t) \approx 1$ and $\sin \phi(t) \approx \phi(t)$. Consequently, $\dot{x} \approx v_0$, representing a ballistic motion for the x -coordinate, with fluctuations $\sigma_x^2 \sim t^4$ [see Eq. (7)] coming from the next order corrections. In contrast, the y -coordinate evolves as $\dot{y} \approx v_0 \phi(t)$. Taking one time-derivative and using Eq. (1c) gives an effective early time evolution for the y -coordinate

$$\ddot{y} \approx \sqrt{2 D_{\text{RAP}}} \eta_\phi(t), \quad \text{where } D_{\text{RAP}} = v_0^2 D_R. \quad (8)$$

This effective Langevin equation then corresponds to the RAP, which has been studied extensively in the literature as one of the simplest possible non-Markovian processes (for reviews see [28–31]). Note that the presence of

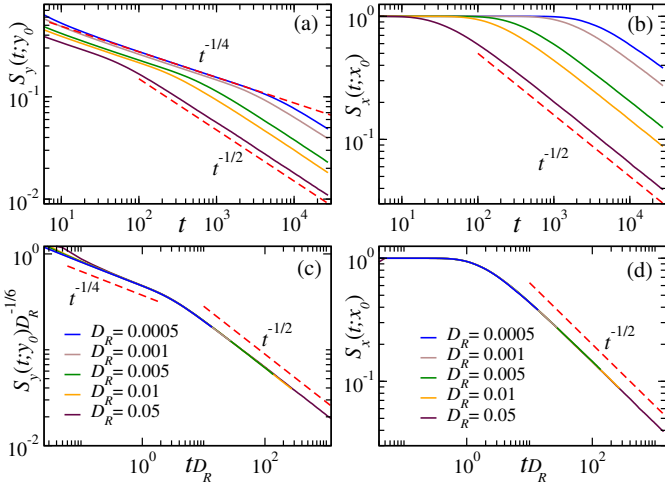


FIG. 4: Persistence probability: Decay of $S_y(t; y_0)$ (a) and $S_x(t; x_0)$ (b) with time for $x_0 = 0, y_0 = 0.1$ in (a) and $x_0 = 0.1, y_0 = 0$ in (b). In (a), $S_y(t)$ initially shows a power law decay $t^{-1/4}$ which crosses over to $t^{-1/2}$ after a time $t \sim D_R^{-1}$. The topmost dashed line is the exact prediction from the RAP, $S_y(t; y_0) \sim t^{-1/4}$ in Eq. (9). (c) Collapse of the curves in (a) according to Eq. (10). (d) Collapse of the curves in (b) following Eq. (12). Here $v_0 = 1$ for all the curves.

the second derivative in time in Eq. (8) makes the process non-Markovian. One hallmark of this non-Markovian nature is an anomalously slow decay of the persistence (and the related first-passage probability). Indeed, it is known that the persistence, *i.e.*, the probability that the process starting at some initial value $y_0 > 0$ does not cross the origin up to time t , decays as a power law $\sim t^{-1/4}$ for large t [28–31], in marked contrast to the standard $\sim t^{-1/2}$ decay for the ordinary Brownian diffusion [29, 30, 32]. Persistence/first-passage properties in active systems have not been explored so much, except very recently in a class of one-dimensional systems [33–36]. The above mapping to the RAP for the y -component of the 2d-ABP signals nontrivial persistence properties in this 2d active system, which we now investigate in detail.

Persistence probability. Let $S_y(t; y_0)$ denote the persistence, *i.e.*, the probability that the y -component of the ABP does not cross $y = 0$ up to time t , starting initially at $y_0 > 0$. To compute $S_y(t; y_0)$, we use the mapping to the RAP, for which the result is known exactly [37] for all y_0 . This result simplifies considerably in the limit $y_0 \rightarrow 0$ (see Eq. (D.7) in [38] where the result was expressed in dimensionless units), to which we focus on here. Translating this result from [38] to our units we get

$$S_y(t; y_0) \simeq \frac{2^{5/6}\Gamma(-4/3)}{3^{2/3}\pi\Gamma(3/4)} \left(\frac{y_0 D_R}{v_0} \right)^{1/6} (t D_R)^{-1/4}. \quad (9)$$

Since the mapping to the RAP holds only for $1 \ll t \ll D_R^{-1}$, we expect this RAP result (9) to hold for the y -component of the ABP only in this time regime. In con-

trast, for $t \gg D_R^{-1}$, we have already shown that the ABP behaves as a standard Brownian motion with diffusion constant $D_{\text{eff}} = v_0^2/(2 D_R)$. Hence, for $t \gg D_R^{-1}$, we would expect $S_y(t; y_0)$ to decay as $t^{-1/2}$. This suggests a crossover from the early time $\sim t^{-1/4}$ to the late time $t^{-1/2}$ decay of $S_y(t; y_0)$, described by the scaling form

$$S_y(t; y_0) = \left(\frac{y_0 D_R}{v_0} \right)^{1/6} \mathcal{F}_y(t D_R), \quad (10)$$

where the crossover scaling function $\mathcal{F}_y(u)$ has the limiting behaviours

$$\mathcal{F}_y(u) \sim \begin{cases} u^{-1/4} & \text{for } u \ll 1 \\ u^{-1/2} & \text{for } u \gg 1. \end{cases} \quad (11)$$

We have verified this scaling form (10) numerically. Figure 4(a) shows $S_y(t; y_0)$ vs. t , obtained from simulations, for different values of D_R . The uppermost dashed line is the exact prediction from Eq. (9). The same data scaled according to Eq. (10) are plotted in Fig 4(c). The excellent data collapse confirms the predicted scaling form (10), along with the asymptotics in Eq. (11).

We have also studied the persistence of the x -component of the ABP denoted by $S_x(t; x_0)$, *i.e.*, the probability that the x -component, starting at $x_0 > 0$, does not cross $x = 0$ up to time t . In this case, at early times $t \ll D_R^{-1}$, $x(t) \approx v_0 t$ with $v_0 > 0$ and therefore $x(t)$ stays positive with probability close to unity. However, at long times $t \gg D_R^{-1}$, $x(t)$ behaves diffusively and we would expect a decay $\sim t^{-1/2}$ for $S_x(t; x_0)$. For simplicity, we consider the limit $x_0 \rightarrow 0$ and in this case, we would expect a crossover of the form

$$S_x(t; x_0) = \mathcal{F}_x(t D_R), \quad (12)$$

where $\mathcal{F}_x(u) \sim 1$ for $u \ll 1$, while $\mathcal{F}_x(u) \sim u^{-1/2}$ for $u \gg 1$. Figures 4(b) and (d) show the behaviour of $S_x(t; x_0)$ for different values of D_R , again a perfect data collapse confirms the predicted crossover in Eq. (12).

Conclusion: In this Letter we have studied the dynamics of an active Brownian particle (ABP) in a 2d harmonic trap. We have demonstrated that the competition between two time scales (the inverse of the rotational diffusion coefficient D_R^{-1} and the inverse of trap strength μ^{-1}) induces a rather interesting and anomalous time evolution. At late times, the dynamics leads to quite different stationary states depending on whether the ABP is strongly passive ($D_R \rightarrow \infty$) or strongly active ($D_R \rightarrow 0$). At short-times, the activity gives rise to highly anisotropic motion – this is reflected in the anomalous $t^{-1/4}$ decay of the persistence probability for the y -coordinate of the ABP. We have established this behaviour using an exact mapping to the random acceleration process (RAP). We expect that this anomalous persistence property of the RAP, which emerges at short times for the 2d-ABP, should be experimentally visible.

Acknowledgments

The authors would like to acknowledge the support from the Indo-French Centre for the promotion of ad-

vanced research (IFCPAR) under Project No. 5604-2.

[1] P. Romanczuk, M. Bär, W. Ebeling, B. Lindner, and L. Schimansky-Geier, *Eur. Phys. J. Special Topics* **202**, 1 (2012).

[2] M. C. Marchetti, J. F. Joanny, S. Ramaswamy, T. B. Liverpool, J. Prost, M. Rao, and R. Aditi Simha, *Rev. Mod. Phys.* **85**, 1143 (2013).

[3] C. Bechinger, R. Di Leonardo, H. Löwen, C. Reichhardt, G. Volpe, and G. Volpe, *Rev. Mod. Phys.* **88**, 045006 (2016).

[4] S. Ramaswamy, *J. Stat. Mech.* 054002 (2017).

[5] É. Fodor, and M. C. Marchetti, [arXiv:1708.08652](https://arxiv.org/abs/1708.08652).

[6] *E. Coli in Motion*, H. C. Berg, (Springer Verlag, Heidelberg, Germany) (2004).

[7] M. E. Cates, *Rep. Prog. Phys.* **75**, 042601 (2012).

[8] X. Trepas, M. R. Wasserman, T. E. Angelini, E. Millet, D. A. Weitz, J. P. Butler, and J. J. Fredberg, *Nature Physics* **5**, 426 (2009).

[9] T. Vicsek, A. Czirók, E. Ben-Jacob, I. Cohen, and O. Shochet, *Phys. Rev. Lett.* **75**, 1226 (1995).

[10] S. Hubbard, P. Babak, S. Th. Sigurdsson, and K. G. Magnússon, *Ecological Modelling*, **174**, 359 (2004).

[11] D. L. Blair, T. Neicu, and A. Kudrolli, *Phys. Rev. E* **67**, 031303 (2003).

[12] L. Walsh, C. G. Wagner, S. Schlossberg, C. Olson, A. Baskaran, and N. Menon, *Soft Matter* **13**, 8964 (2017).

[13] J. Palacci, S. Sacanna, A. P. Steinberg, D. J. Pine, and P. M. Chaikin, *Science* **339**, 936 (2013).

[14] J. Toner, Y. Tu, and S. Ramaswamy, *Ann. of Phys.* **318**, 170 (2005).

[15] N. Kumar, H. Soni, S. Ramaswamy, and A. K. Sood, *Nature Comm.* **5**, 4688 (2014).

[16] Y. Fily, and M. C. Marchetti, *Phys. Rev. Lett.* **108**, 235702 (2012).

[17] A. B. Slowman, M. R. Evans, and R. A. Blythe, *Phys. Rev. Lett.* **116**, 218101 (2016).

[18] J. Schwarz-Linek, C. Valeriani, A. Cacciuto, M. E. Cates, D. Marenduzzo, A. N. Morozov, and W. C. K. Poon, *Proc. Natl. Acad. Sci. USA* **109**, 4052 (2012).

[19] G. S. Redner, M. F. Hagan, and A. Baskaran, *Phys. Rev. Lett.* **110**, 055701 (2013).

[20] J. Stenhammar, R. Wittkowski, D. Marenduzzo, and M. E. Cates, *Phys. Rev. Lett.* **114**, 018301 (2015).

[21] A. P. Solon, Y. Fily, A. Baskaran, M. E. Cates, Y. Kafri, M. Kardar, and J. Tailleur, *Nature Physics* **11**, 673 (2015).

[22] S. C. Takatori, R. De Dier, J. Vermant, and J. F. Brady, *Nature Comm.* **7**, 10694 (2016).

[23] M. E. Cates, and J. Tailleur, *Europhys. Lett.* **101**, 20010 (2013).

[24] A. Pototsky, and H. Stark, *Europhys. Lett.* **98**, 50004 (2012).

[25] A. P. Solon, M. E. Cates, and J. Tailleur, *Eur. Phys. J. Special Topics* **224**, 1231 (2015).

[26] See Supplemental Material for the details.

[27] D. Gredat, I. Dornic, and J. M. Luck, *J. Phys. A: Math. Theor.* **44**, 175003 (2011).

[28] T. W. Burkhardt, *J. Stat. Mech.* P07004 (2007).

[29] S. N. Majumdar, *Curr. Sci.* **77**, 370 (1999).

[30] A. J. Bray, S. N. Majumdar, and G. Schehr, *Adv. in Phys.* **62**, 225 (2013).

[31] T. W. Burkhardt, *First Passage of a Randomly Accelerated Particle in First-Passage Phenomena and Their Applications*, edited by R. Metzler, G. Oshanin, and S. Redner (World Scientific, 2014).

[32] *A Guide to First-Passage Processes*, S. Redner, Cambridge University Press (2001).

[33] L. Angelani, R. Di Leonardo, and M. Paoluzzi, *Euro. J. Phys. E* **37**, 59 (2014).

[34] K. Malakar, V. Jemseena, A. Kundu, K. Vijay Kumar, S. Sabhapandit, S. N. Majumdar, S. Redner, and A. Dhar, [arXiv:1711.08474](https://arxiv.org/abs/1711.08474).

[35] A. Scacchi, and A. Sharma, *Mol. Phys.* **116**, 460 (2017).

[36] T. Demaerel, and C. Maes, *Phys. Rev. E* **97**, 032604 (2018).

[37] T. W. Burkhardt, *J. Phys. A: Math. Gen.* **26**, L1157 (1993).

[38] S. N. Majumdar, A. Rosso, and A. Zoia, *J. Phys. A: Math. Theor.* **43**, 115001 (2010).

Supplemental Material for “Active Brownian Motion in Two Dimensions”

Effective Noise: The Langevin equation (2) in the main text reads

$$\dot{z} = -\mu z + \xi(t) \quad (\text{S1})$$

where $\xi(t) = v_0 e^{i\phi(t)}$. Here, $\phi(t)$ is a Brownian motion with a diffusion constant D_R [see Eq. (1) in the main text] and starting from $\phi(0) = 0$. Clearly, $\phi(t)$ is a Gaussian process with two-point correlation

$$\langle \phi(t_1) \phi(t_2) \rangle = 2 D_R \min(t_1, t_2). \quad (\text{S2})$$

Since $\xi(t) = v_0 e^{i\phi(t)}$, the noise $\xi(t)$ is bounded in time, even though $\phi(t)$ grows with time as $\phi(t) \sim \sqrt{D_R t}$. The one and two-point correlation functions of the noise $\xi(t)$ can be computed using the fact that $\phi(t)$ is a Gaussian process. In fact, we will use a well known identity for a Gaussian process $\phi(t)$,

$$\left\langle \exp \left(i \sum_j a_j \phi(t_j) \right) \right\rangle = \exp \left(-\frac{1}{2} \sum_{j,k} a_j a_k \langle \phi(t_j) \phi(t_k) \rangle \right) \quad (\text{S3})$$

where a_i 's are arbitrary. The average $\langle \xi(t) \rangle$ is thus given by

$$\langle \xi(t) \rangle = v_0 \langle e^{i\phi(t)} \rangle = v_0 e^{-D_R t}, \quad (\text{S4})$$

where we used Eq. (S3) with $a_1 = 1$ (and $t_1 = t$), $a_j = 0$ for $j > 1$ and $\langle \phi^2(t) \rangle = 2D_R t$. Similarly the two-point functions can be obtained in a straightforward manner from Eq. (S3) by appropriately choosing a_1 and a_2 and keeping $a_j = 0$ for $j > 2$. We get

$$\langle \xi(t_1) \xi(t_2) \rangle = \langle \bar{\xi}(t_1) \bar{\xi}(t_2) \rangle \quad (\text{S5})$$

$$= v_0^2 \exp[-D_R (t_1 + t_2 + 2 \min(t_1, t_2))] \quad (\text{S6})$$

where $\bar{\xi}(t) = v_0 e^{-i\phi(t)}$ is the complex conjugate of $\xi(t)$. Similarly we also obtain

$$\langle \xi(t_1) \bar{\xi}(t_2) \rangle = \langle \bar{\xi}(t_1) \xi(t_2) \rangle \quad (\text{S7})$$

$$= v_0^2 \exp[-D_R |t_1 - t_2|]. \quad (\text{S8})$$

This result is quoted as Eq. (3) in the main text. Therefore one sees that the noise $\xi(t)$ appearing in the Langevin equation (S1), has a finite correlation time D_R^{-1} , *i.e.*, a finite memory. This makes $z(t)$ a non-Markovian process.

Fokker-Planck Equation: Let $\mathcal{P}(x, y, \phi, t)$ denote the probability that at any time t , the ABP has a position (x, y) and orientation ϕ . $\mathcal{P}(x, y, \phi, t)$ evolves according to a Fokker-Planck equation,

$$\partial_t \mathcal{P}(x, y, \phi; t) = \frac{\partial}{\partial x} \left[(\mu x - v_0 \cos \phi) \mathcal{P} \right]$$

$$+ \frac{\partial}{\partial y} \left[(\mu y - v_0 \sin \phi) \mathcal{P} \right] + D_R \frac{\partial^2 \mathcal{P}}{\partial \phi^2}, \quad (\text{S9})$$

where have suppressed the argument of \mathcal{P} on the right hand side for brevity. The marginal probability distribution of the position can then be obtained by integrating over ϕ ,

$$P(x, y, t) = \int d\phi \mathcal{P}(x, y, \phi, t). \quad (\text{S10})$$

In the long time limit the position distribution $P(x, y, t)$ converges to a stationary form which is denoted by

$$P_{\text{stat}}(x, y) = P(x, y, t \rightarrow \infty). \quad (\text{S11})$$

While the Fokker-Planck equation (S9) is exact, unfortunately it is not easy to solve it explicitly. We will see later however that one can actually derive explicit results for the moments of this probability distribution, at least in some limiting cases. The probability distribution $P(x, y, t)$ in cartesian coordinates can also be expressed in the radial coordinates as $P(r, \theta, t)$. For later purposes, we define the marginal radial distribution $P_{\text{rad}}(r, t)$ as

$$P_{\text{rad}}(r, t) = \int_0^{2\pi} P(r, \theta, t) d\theta. \quad (\text{S12})$$

Note that the normalisation of the total probability translates to

$$\int_0^\infty r P_{\text{rad}}(r, t) dr = 1. \quad (\text{S13})$$

Mean-squared displacements: The mean-squared displacement of the ABP can be exactly calculated from the Langevin equations (1) or (2) in the main text. The Langevin equation (2) in the text, for $\mu = 0$, reads

$$z(t) = \int_0^t ds \xi(s) \quad (\text{S14})$$

where $z = x + iy$, $\xi(s) = v_0 e^{i\phi(s)}$ is the effective noise mentioned above. The first two moments of the process $z(t)$ at a given time t read

$$\langle z(t) \rangle = \int_0^t \langle \xi(s) \rangle ds \quad (\text{S15})$$

$$\langle z^2(t) \rangle = \int_0^t ds_1 \int_0^t ds_2 \langle \xi(s_1) \xi(s_2) \rangle \quad (\text{S16})$$

$$\langle \bar{z}^2(t) \rangle = \int_0^t ds_1 \int_0^t ds_2 \langle \bar{\xi}(s_1) \bar{\xi}(s_2) \rangle \quad (\text{S17})$$

$$\langle z(t) \bar{z}(t) \rangle = \int_0^t ds_1 \int_0^t ds_2 \langle \xi(s_1) \bar{\xi}(s_2) \rangle. \quad (\text{S18})$$

Using the one and two-point correlation functions of $\xi(t)$ in Eqs. (S4)-(S8), one can easily work out these moments of $z(t)$. We get, for example,

$$\langle z(t) \rangle = \langle \bar{z}(t) \rangle = \frac{v_0}{D_R} (1 - e^{-D_R t}) . \quad (\text{S19})$$

The mean of the x and the y component follows immediately

$$\langle x(t) \rangle = \frac{1}{2} \langle z + \bar{z} \rangle = \frac{v_0}{D_R} (1 - e^{-D_R t}) \quad (\text{S20})$$

$$\langle y(t) \rangle = \langle z - \bar{z} \rangle / 2 = 0 . \quad (\text{S21})$$

Similarly, the variances of x and y can also be computed

$$\begin{aligned} \sigma_x^2 &= \langle x^2 \rangle - \langle x \rangle^2 = \frac{1}{4} [\sigma_z^2 + \sigma_{\bar{z}}^2 + 2\langle z\bar{z} \rangle - 2\langle z \rangle \langle \bar{z} \rangle] \\ \sigma_y^2 &= \langle y^2 \rangle = \frac{1}{4} [\langle z^2 \rangle + \langle \bar{z}^2 \rangle - 2\langle z\bar{z} \rangle] \end{aligned} \quad (\text{S22})$$

where $\sigma_z^2 = \langle z^2 \rangle - \langle z \rangle^2$ and $\sigma_{\bar{z}}^2 = \langle \bar{z}^2 \rangle - \langle \bar{z} \rangle^2$. Explicitly evaluating the integrals in (S15) leads to,

$$\begin{aligned} \sigma_x^2 &= \frac{v_0^2}{D_R} t + \frac{v_0^2}{12D_R^2} [e^{-4D_R t} - 12e^{-2D_R t} + 32e^{-D_R t} - 21] \\ \sigma_y^2 &= \frac{v_0^2}{D_R} t - \frac{v_0^2}{12D_R^2} [e^{-4D_R t} - 16e^{-D_R t} + 15] . \end{aligned} \quad (\text{S23})$$

At long times $t \gg D_R^{-1}$, both σ_x^2 and σ_y^2 grow linearly with time with an effective diffusion constant $D_{\text{eff}} = v_0^2/(2D_R)$. In contrast, at short-times $t \ll D_R^{-1}$, expanding (S23) in Taylor series, we find

$$\begin{aligned} \sigma_x^2 &\approx \frac{1}{3} v_0^2 D_R^2 t^4 - \frac{7}{15} v_0^2 D_R^3 t^5 + \dots \\ \sigma_y^2 &\approx \frac{2}{3} v_0^2 D_R t^3 - \frac{5}{6} v_0^2 D_R^2 t^4 + \dots \end{aligned} \quad (\text{S24})$$

which gives the results in Eq. (9) of the main text. These results reflect a strong anisotropy at early times in the (x, y) plane since, for small t , $\sigma_y^2 \sim t^3 \gg \sigma_x^2 \sim t^4$.

Time-evolution in a harmonic trap and a statistical recursion relation: In the presence of the harmonic trap, the position of an ABP, expressed in terms of $z = x + iy$ evolves following the linear Langevin equation (2) in the main text. Integrating this equation one gets

$$z(t) = v_0 \int_0^t ds e^{-\mu(t-s)} e^{i\phi(s)} \quad (\text{S25})$$

where $\phi(s)$ is a standard Brownian motion with diffusion constant D_R and starting at $\phi(0) = 0$. Our goal is to evaluate the moment of the type

$$M_{k,l}(t) = \langle z^k(t) \bar{z}^l(t) \rangle . \quad (\text{S26})$$

In principle, one can use Eq. (S25) and the Gaussian property (S3), to express $M_{k,l}(t)$ as a $(k + l)$ -fold multiple integral. However, evaluating this multiple integral

explicitly seems very hard. Instead, we will derive below an exact recursion relation for the moments $M_{k,l}(t)$.

In fact, to derive such a recursion relation, we find it useful to use the Kesten variable representation used by Gredat, Dornic, Luck (GDL) in Ref. [1] in a different context. Indeed, GDL were interested in the imaginary exponential functional of a Brownian motion and studied an effective process given by

$$z^{GDL}(t) = v_0 \int_0^t e^{-\mu s + i\phi(s)} ds . \quad (\text{S27})$$

These two processes, $z(t)$ in (S25) and $z^{GDL}(t)$ in (S27), look deceptively similar. However it turns out that they have rather different properties and in fact the recursion relation for the moments turn out to be rather different.

To derive these recursion relations, it is useful to first recast the continuous time expression (S25) in a discrete-time setting. We imagine the interval $[0, t]$ consists of n discrete intervals each of length $\varepsilon > 0$, such that $t = n\varepsilon$. We then split the time interval $[0, t]$ in the integral in Eq. (S25) into two separate intervals $[0, \varepsilon]$ and $[\varepsilon, t]$. This gives

$$z(t) = v_0 \left(\int_0^\varepsilon e^{-\mu(t-s)+i\phi(s)} ds + \int_\varepsilon^t e^{-\mu(t-s)+i\phi(s)} ds \right) . \quad (\text{S28})$$

The first integral, to leading order in ε , gives $e^{-\mu t} \varepsilon$, where we used $\phi(0) = 0$. In the second integral, we make a change of variable $s = \varepsilon + \tau$ and rewrite it as, $\int_0^{t-\varepsilon} e^{-\mu(t-\varepsilon-\tau)+i\phi(\varepsilon+\tau)} d\tau$. Next we write $\phi(\varepsilon + \tau) = \phi(\varepsilon + \tau) - \phi(\varepsilon) + \phi(\varepsilon)$, i.e., add and subtract $\phi(\varepsilon)$. Putting this together, we get

$$z(t) \approx v_0 \left(e^{-\mu t} \varepsilon + e^{i\phi(\varepsilon)} \int_0^{t-\varepsilon} e^{-\mu(t-\varepsilon-\tau)+i\tilde{\phi}(\tau)} d\tau \right) , \quad (\text{S29})$$

where

$$\tilde{\phi}(\tau) = \phi(\varepsilon + \tau) - \phi(\varepsilon) . \quad (\text{S30})$$

Now we will use the crucial property that $\tilde{\phi}(\tau)$ is also a Brownian motion starting at $\tilde{\phi}(0) = 0$, and with correlation function $\langle \tilde{\phi}(t_1) \tilde{\phi}(t_2) \rangle = 2D_R \min(t_1, t_2)$. Importantly, the statistical properties of $\tilde{\phi}(t)$ do not depend on ε . In other words, one can write a statistical identity in law

$$\tilde{\phi}(\tau) \equiv \phi(\tau) , \quad (\text{S31})$$

where \equiv means that the right hand side and left hand side have identical distributions. Consequently, using this identity (S31) and the definition of $z(t)$ in Eq. (S25), the integral

$$\int_0^{t-\varepsilon} e^{-\mu(t-\varepsilon-\tau)+i\tilde{\phi}(\tau)} d\tau \equiv z(t - \varepsilon) . \quad (\text{S32})$$

Hence, (S29) provides us with a statistical identity

$$z(t) \equiv v_0 \varepsilon e^{-\mu t} + e^{i\phi(\varepsilon)} z(t - \varepsilon) . \quad (\text{S33})$$

Denoting $z_n = z(t = n\varepsilon)$ in the discrete-time setting, we then obtain a Kesten type statistical recursion relation

$$z_n \equiv v_0 \varepsilon e^{-\mu n\varepsilon} + \eta_n z_{n-1} \quad (\text{S34})$$

where $\eta_n = e^{i\phi(\varepsilon)}$ is an effective noise, independent of z_{n-1} . Using the Gaussian property of $\phi(s)$ (S3), one can easily evaluate the moments of the noise η_n . For instance, one gets $\langle \eta_n \rangle = e^{-\varepsilon D_R}$ and correlation $\langle \eta_n^k \bar{\eta}_n^l \rangle = e^{-\varepsilon D_R(k-l)^2}$, where $\bar{\eta}_n = e^{-i\phi(\varepsilon)}$ is the complex conjugate of η_n . Note that in the case of z^{GDL} in Eq. (S27), by following a similar scheme, one would instead get the recursion relation [1]

$$z_n^{GDL} \equiv v_0 \varepsilon + e^{-\mu \varepsilon} \eta_n z_{n-1}^{GDL}, \quad (\text{S35})$$

which is manifestly different from our recursion relation (S34).

An exact recursion relation for the moments. We start with the discrete-time recursion relation (S34), together with its complex conjugate which reads

$$\bar{z}_n = v_0 \varepsilon e^{-\mu \varepsilon} + \bar{\eta}_n \bar{z}_{n-1}. \quad (\text{S36})$$

Let us denote the moment $M_{k,l}(n) = \langle z_n^k \bar{z}_n^l \rangle$. We take z_n^k in Eq. (S34) and \bar{z}_n^l in Eq. (S36), multiply them and then take the expectation value with respect to the noise η_n . We use the independence of η_n and z_{n-1} and the known moments of the noise η_n and then expand in powers of ε . Keeping terms only up to order $O(\varepsilon)$, we get

$$\begin{aligned} M_{k,l}(n) \simeq & [1 - \varepsilon D_R(k-l)^2] M_{k,l}(n-1) \\ & + v_0 \varepsilon e^{-\mu n \varepsilon} [k M_{k-1,l}(n-1) + l M_{k,l-1}(n-1)]. \end{aligned} \quad (\text{S37})$$

Taking the continuous-time limit $\varepsilon \rightarrow 0$ and replacing $(M_{k,l}(n) - M_{k,l}(n-1))/\varepsilon$ by the time derivative $dM_{k,l}/dt$ we arrive at the exact recursion relation

$$\dot{M}_{k,l} = -D_R(k-l)^2 M_{k,l} + v_0 e^{-\mu t} [k M_{k-1,l} + l M_{k,l-1}] \quad (\text{S38})$$

with the conditions $M_{0,0}(t) = 1$ at all times and $M_{k,l}(0) = 0$ for $k, l > 0$. This gives Eq. (4) of the

main text. Note that, since the right hand side is explicitly time-dependent, it is not possible to obtain the stationary state by simply equating $\dot{M}_{k,l}$ to zero, rather one has to find the full time-dependent solution and then take long-time limit to find the same. In contrast, for the GDL case, the corresponding recursion relation for the moments $\tilde{M}_{k,l}(t) = M_{kl}^{GDL}(t)$ is given by [1]

$$\begin{aligned} \frac{d}{dt} \tilde{M}_{k,l} = & -(\mu(k+l) + D_R(k-l)^2) \tilde{M}_{k,l} \\ & + v_0 (k \tilde{M}_{k-1,l} + l \tilde{M}_{k,l-1}). \end{aligned} \quad (\text{S39})$$

Note that there is no explicit time dependence on the right hand side of this equation (S39) and the moments in the stationary state can be simply obtained by setting the time derivative to be zero on the left hand side of (S39). As mentioned above, the situation in our case is completely different.

Solution of the moment recursion relation. Consider the time dependent recursion relation in (S38). We can think of (k, l) as the grid points on the $2d$ lattice with $k, l \geq 0$. We note that by definition $M_{0,0}(t) = 1$ at all times t . As a result, it is easy to see from the recursion relation (S38) that the solution $M_{k,l}(t)$ is symmetric under exchange of k and l , *i.e.*,

$$M_{k,l}(t) = M_{l,k}(t). \quad (\text{S40})$$

Hence, it is sufficient to study $M_{k,l}(t)$ only for $k \geq l$. The recursion relations for the first few values of k and l read, for instance (with the convention that $M_{k,l}(t) = 0$ for $k, l < 0$)

$$\begin{aligned} \dot{M}_{1,0}(t) &= -D_R M_{1,0}(t) + v_0 e^{-\mu t} M_{0,0}(t) \\ \dot{M}_{1,1}(t) &= 2v_0 e^{-\mu t} M_{1,0}(t) \\ \dot{M}_{2,0}(t) &= -4D_R M_{2,0}(t) + 2v_0 e^{-\mu t} M_{1,0}(t) \end{aligned} \quad (\text{S41})$$

and so on. These equations can be solved recursively, *i.e.*, using the solution of the previous equation. The solution of these first few moments can be written explicitly at all times t ,

$$\begin{aligned} M_{1,0}(t) &= \frac{v_0 (e^{-\mu t} - e^{-D_R t})}{D_R - \mu} \\ M_{1,1}(t) &= \frac{v_0^2}{(D_R - \mu)} \left[\frac{1 - e^{-2\mu t}}{\mu} - \frac{2(1 - e^{-(D_R + \mu)t})}{D_R + \mu} \right] \\ M_{2,0}(t) &= \frac{v_0^2 [(3D_R - \mu)e^{-2\mu t} - 2(2D_R - \mu)e^{-(D_R + \mu)t} + (D_R - \mu)e^{-4D_R t}]}{(D_R - \mu)(2D_R - \mu)(3D_R - \mu)}. \end{aligned} \quad (\text{S42})$$

As we see, the solutions quickly become long and cumber-

some as k and l increase. To extract more specific infor-

mations, we now investigate two limiting cases ($D_R \rightarrow \infty$ and $D_R = 0$) where $M_{k,l}(t)$ can be obtained explicitly for all k and l .

Strongly passive limit ($D_R \rightarrow \infty$): To solve the moment evolution Eq. (S38) in the limit of $D_R \rightarrow \infty$ we inspect the large D_R behaviour of the first few moments presented in Eq. (S42) above. It turns out that these quantities, to the leading order in $1/D_R$, are of the form,

$$M_{k,l}(t) \simeq \frac{v_0^{k+l} k!}{[(k-l)!]^2} \left[\frac{e^{-\mu t}}{D_R} \right]^k \left[\frac{e^{\mu t} - e^{-\mu t}}{\mu} \right]^l, \quad k \geq l. \quad (\text{S43})$$

Indeed, substituting this ansatz in the recursion relation (S38), it can be verified that Eq. (S38) is indeed satisfied by Eq. (S43), up to leading order for large D_R . Note that this leading order result for $M_{k,l}(t)$ in Eq. (S43) is actually valid for all time t , including $t = 0$.

To extract further information, we consider the diagonal moments $M_{k,k}(t) = \langle (z(t)\bar{z}(t))^k \rangle$. Using $z(t)\bar{z}(t) = x^2(t) + y^2(t) = r^2(t)$, the diagonal element $M_{k,k}(t) = \langle r^{2k}(t) \rangle$ is precisely the $2k$ -th radial moment of the full distribution. In terms of the marginal radial distribution $P_{\text{rad}}(r, t)$ defined in Eq. (S12), this moment reads

$$\langle r^{2k}(t) \rangle = \int_0^\infty r^{2k+1} P_{\text{rad}}(r, t) dr. \quad (\text{S44})$$

Setting $l = k$ in Eq. (S43) we then get

$$\langle r^{2k}(t) \rangle = M_{k,k}(t) \simeq \Gamma(k+1) \left[\frac{v_0^2}{\mu D_R} (1 - e^{-2\mu t}) \right]^k. \quad (\text{S45})$$

Anticipating a Gaussian behaviour for the radial distribution, we make the ansatz, and check a posteriori, that $P_{\text{rad}}(r, t)$ has the form $P_{\text{rad}}(r, t) = A(t) e^{-B(t)r^2}$. Substituting this ansatz in Eq. (S44) and comparing to the result in (S43), we see that

$$A(t) = 2B(t), \quad B(t) = \frac{\mu D_R}{v_0^2 (1 - e^{-2\mu t})}. \quad (\text{S46})$$

Finally, this gives

$$P_{\text{rad}}(r, t) \simeq \frac{2\mu D_R}{v_0^2 (1 - e^{-2\mu t})} \exp \left[-\frac{\mu D_R r^2}{v_0^2 (1 - e^{-2\mu t})} \right]. \quad (\text{S47})$$

which is quoted as Eq. (5) in the main text.

Note that, from Eq. (S43) it follows that for $k \neq l$, $M_{k,l}(t)$ decays exponentially with time and vanishes in the long time limit. This indicates that the distribution quickly loses the anisotropy and the stationary distribution becomes radially symmetric. Consequently, the stationary position distribution in Eq. (S11) is given by

$$P_{\text{stat}}(x, y) = \frac{1}{2\pi} P_{\text{rad}}(r, t \rightarrow \infty). \quad (\text{S48})$$

Using Eq. (S47), one gets the expected Boltzmann distribution

$$P_{\text{stat}}(x, y) = \frac{\mu D_R}{\pi v_0^2} \exp \left[-\frac{\mu D_R (x^2 + y^2)}{v_0^2} \right]. \quad (\text{S49})$$

Note however that our result in Eq. (S47) contains the full time-dependent solution (and not just the stationary limit) for the radial part of the position distribution function.

Strongly active limit ($D_R = 0$): In this case, the first term on the rhs of Eq. (S38) drops out and it can be checked that

$$M_{k,l}(t) = \left[\frac{v_0}{\mu} (1 - e^{-\mu t}) \right]^{k+l} \quad (\text{S50})$$

solves the resulting equation at all times t . Again, setting $l = k$ in (S50) the time-dependent radial moments are given by

$$\langle r^{2k}(t) \rangle = M_{k,k}(t) = \left[\frac{v_0}{\mu} (1 - e^{-\mu t}) \right]^{2k}. \quad (\text{S51})$$

Comparing Eq. (S44) with Eq. (S51) gives the time-dependent marginal radial distribution,

$$P_{\text{rad}}(r, t) = \frac{\mu}{v_0 (1 - e^{-\mu t})} \delta \left[r - \frac{v_0 (1 - e^{-\mu t})}{\mu} \right]. \quad (\text{S52})$$

Note however that strictly for $D_R = 0$, the position distribution $P(x, y, t)$ is not radially symmetric. Indeed, in this case, the Langevin equation (1) in the main text reduces to a pair of deterministic equations:

$$\dot{x} = -\mu x + v_0 \quad \text{and} \quad \dot{y} = -\mu y, \quad (\text{S53})$$

with initial conditions $x(0) = y(0) = 0$. Solving these equations give $x(t) = (v_0/\mu)(1 - e^{-\mu t})$ and $y(t) = 0$. Consequently, the position distribution function is given by

$$P(x, y, t) = \delta \left(x - \frac{v_0 (1 - e^{-\mu t})}{\mu} \right) \delta(y). \quad (\text{S54})$$

One can check that the moment $M_{k,l}(t)$ computed with this distribution is indeed given by (S50). Moreover, the radial marginal distribution $P_{\text{rad}}(r, t)$ computed from this two-dimensional distribution is indeed given by (S52).

Thus strictly for $D_R = 0$ the position distribution in the $2d$ -plane is highly anisotropic. This is true even in the $t \rightarrow \infty$ limit, where we see from Eq. (S50) that

$$M_{k,l}(t \rightarrow \infty) = \left(\frac{v_0}{\mu} \right)^{k+l} \quad \text{for all } k, l. \quad (\text{S55})$$

Thus, the off-diagonal elements remain non-zero as $t \rightarrow \infty$, indicating the presence of anisotropy in the stationary state.

However, for any finite $D_R > 0$, the rotational diffusion spreads the particle position uniformly over the angle $[0, 2\pi]$. Consequently, in the long time limit and $D_R \rightarrow 0^+$, the position distribution approaches a stationary form that is fully isotropic in the $2d$ plane. Indeed, from the exact expression for the moments in (S42), it

is easy to verify that, for $D_R \rightarrow 0^+$, the off-diagonal elements decay as $M_{k,l}(t) \sim e^{-D_R(k-l)^2 t}$ at late times, for $k \neq l$. In particular, for $t \gg D_R^{-1}$, $M_{k,l}(t) \rightarrow 0$ for $k \neq l$. In contrast, the diagonal elements approach to non-zero values as $t \rightarrow \infty$. More precisely, we find

$$\begin{aligned} M_{k,k}(t \rightarrow \infty) &\rightarrow \left(\frac{v_0}{\mu}\right)^{2k} \\ M_{k,l}(t \rightarrow \infty) &\rightarrow 0, \quad k \neq l \end{aligned} \quad (\text{S56})$$

Note the difference with the strictly $D_R = 0$ case in

Eq. (S55). Consequently, in this $D_R \rightarrow 0^+$ limit, for $t \gg D_R^{-1}$, it follows from Eq. (S56) that the position distribution approaches an isotropic form in the stationary limit and is given by

$$P_{\text{stat}}(x, y) = \frac{\mu}{2\pi v_0} \delta \left[\sqrt{x^2 + y^2} - \frac{v_0}{\mu} \right] \quad (\text{S57})$$

which is equivalent to Eq. (8) in the main text.

[1] D. Gredat, I. Dornic, J. M. Luck, J. Phys. A: Math. Theor. **44**, 175003 (2011).